Supporting information

Modeling High-Pressure Hydrogen Uptake by Nanoporous Metal-Organic Frameworks: Implications for Hydrogen Storage and Delivery

Pamela Ramirez-Vidal, Rafael L. S. Canevesi, Alain Celzard, Vanessa Fierro*

Université de Lorraine, CNRS, IJL, 88000 Epinal, France

* Corresponding author. Tel: + 33 329 29 61 77.

Fax: + 33 329 29 61 38.

E-mail address: Vanessa.Fierro@univ-lorraine.fr (V. Fierro)

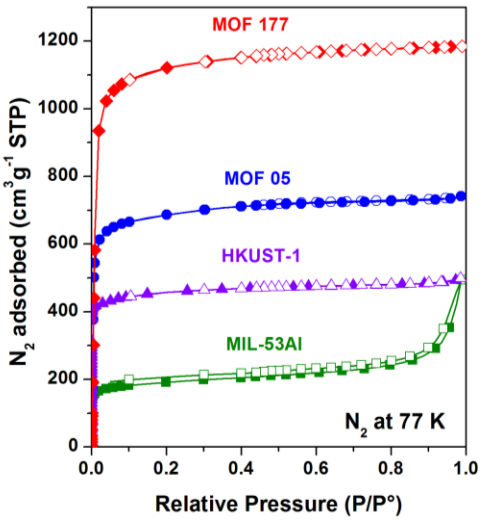

Figure S1. N_2 adsorption isotherms of the MOFs considered in this study at 77 K up to 0.1 MPa.

Table S1. Results of the textural characterization of the samples.

Method	Parameter[a]	MIL-53 Al	MOF-5	HKUST-1	MOF-177
BET [1] N_2 at 77 k	$A_{BET\,N2}$ ($m^2\ g^{-1}$)	727	2775	1882	4557
	$A_{BET\,Ar}$ ($m^2\ g^{-1}$)	681	2589	1903	4215
V_T at $p/p°$=0.97	$V_{T\,N2}$ ($cm^3\ g^{-1}$)	0.62	1.14	0.76	1.84
	$V_{T\,Ar}$ ($cm^3\ g^{-1}$)	0.43	1.05	0.73	1.66
Dubinin-Astakov [2]	$V_{DA\,Ar}$ ($cm^3\ g^{-1}$)	0.25	0.96	0.73	1.42
	n (fitted)	2.00	1.28	2.00	1.27
NLDFT [3–5] Ar at 87 K	S_{NLDFT} ($m^2\ g^{-1}$)	1666	3280	4061	3987
	$S_{(<0.7)\,NLDFT}$ ($m^2\ g^{1}$)	668	267	1136	32
	$S_{(0.7\text{-}2nm)NLDFT}$ ($m^2\ g^{-1}$)	1607	3280	4061	3756
	$V_{T\,NLDFT}$ ($cm^3\ g^{-1}$)	0.43	1.06	0.78	1.66
	V_{meso} ($cm^3\ g^{-1}$)	0.15	0.00	0.00	0.12
	V_{micro} ($cm^3\ g^{-1}$)	0.28	1.06	0.78	1.54
	$V_{(< 0.7nm)}$ ($cm^3\ g^{-1}$)	0.130	0.029	0.160	0.003
	$V_{(0.7\text{-}2\ nm)}$ ($cm^3\ g^{-1}$)	0.152	1.03	0.62	1.54
	$\bar{d}_T$ (nm)	6.26	1.29	0.81	1.66
	$\bar{d}_\mu$ (nm)	0.72	1.29	0.77	1.65
Density	ρ_{sk} ($g\ cm^{-3}$)	1.629	2.007	2.212	1.728
	ρ_{TAP} ($g\ cm^{-3}$)	0.394	0.345	0.373	0.264
	ρ_{cry} ($g\ cm^{-3}$)	0.978 [6]	0.590 [7,8]	0.879[9]	0.430 [8,10,11]
	$0.74\rho_{cry}$ ($g\ cm^{-3}$)	0.724	0.437	0.650	0.318

[a] A_{BET} is the surface area calculated by applying the BET equation to the nitrogen and argon adsorption isotherms. The total pore volumes $V_{T\,N2}$ and $V_{T\,Ar}$ were determined from the adsorption isotherms at $p/p°$=0.97. The micropore volume V_{DA} was calculated using the Dubinin- Astakhov equation. The 2D-NLDFT-HS model was the cylindrical pore (Me-type zeolite) applied to Ar

sorption data (87 K). The micropore ($\bar{d}_\mu$) and total ($\bar{d}_T$) average pore sizes were calculated from the PSDs and were volume-weighed.

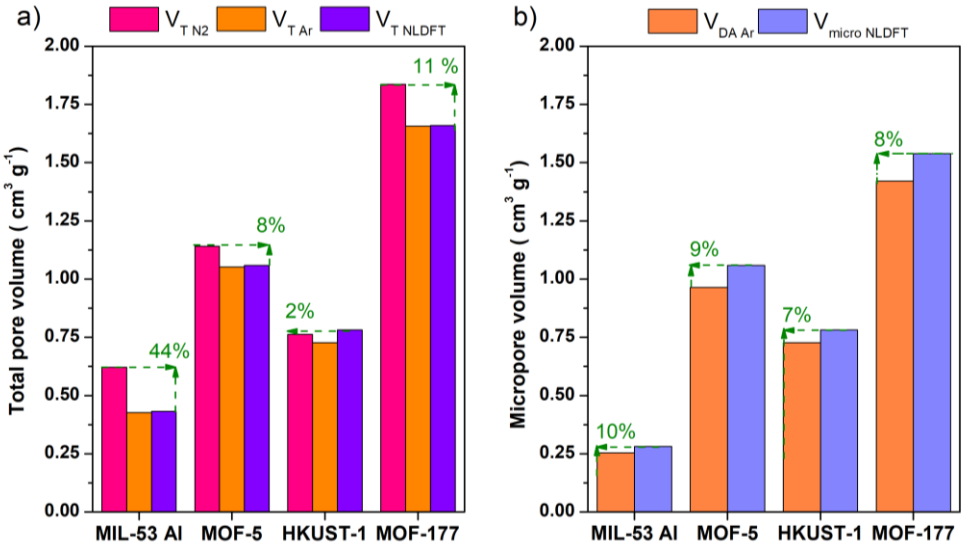

Figure S2. a) Comparison between the total pore volume calculated from the N_2 and Ar adsorption data at $p/p°$=0.97 and that obtained by fitting the Ar data with the NLDFT model; b) Comparison of the micropore volume obtained by the DA and NLDFT models using Ar adsorption. Percentage differences (green values) were calculated using the volumes based on the NLDFT model and are displayed in green.

Table S2. H_2 and CO_2 gravimetric and volumetric uptakes at 77 K and 273 K, and up to 0.1 MPa.

Sample	**Gravimetric**	**Gravimetric**	**Volumetric**	**Volumetric**
	H_2	CO_2	H_2	CO_2
	77 K and 0.1 MPa	273 K and 0.1 MPa	77 K and 0.1 MPa	273 K and 0.1 MPa
	(wt.%)	(wt.%)	(g L^{-1})	(g L^{-1})
MIL-53 Al	1.3	16.9	5.2	66.7
MOF-5	1.2	6.4	4.1	22.1
HKUST-1	2.5	41.8	9.5	155.9
MOF-177	1.3	6.6	3.4	17.4

Table S3. Henry's law constants of MOFs for H_2 and CO_2 adsorption at 77 and 273 K in the indicated pressure range.

Sample	**H_2 at 77 K**			**CO_2 at 273 K**		
	Range of pressure	R^2	$K_{H\,H2}$	Range of pressure	R^2	$K_{H\,CO2}$
	(kPa)		(wt.% kPa^{-1})	(kPa)		(wt.% kPa^{-1})
MIL-53 Al	0.134-3.319	0.993	0.05	0.139-5.718	0.988	0.53
MOF-5	0.252-7.64	0.995	0.03	0.412-10.218	0.988	0.08
HKUST-1	0.093-4.289	0.986	0.14	0.254-10.952	0.999	0.68
MOF-177	0.291-8.318	0.997	0.02	0.428-11.546	0.995	0.07

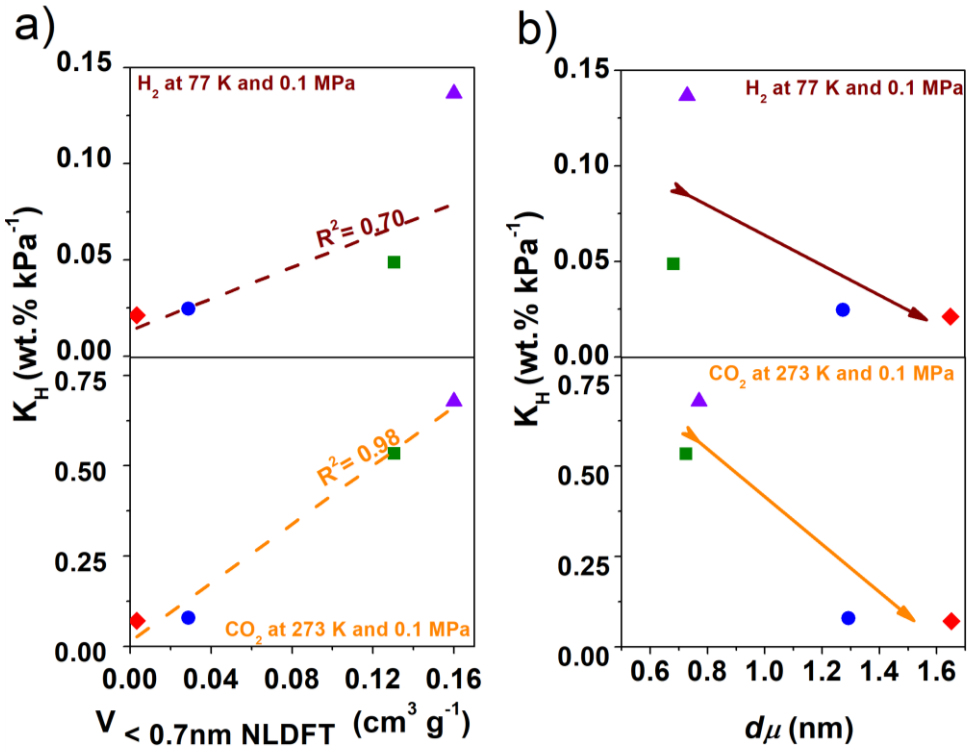

Figure S3. Henry's law constants for CO_2 and H_2 adsorption at 0.1 MPa and 273 or 77 K, plotted against: (a) $V_{<0.7\ NLDFT}$; and (b) the average micropore size of the samples.

Table S4. Excess H_2 uptake at 77 K and 2-3 MPa for the four MOFs.

		Excess H_2 uptake at 77 K and 2-3 MPa		
Sample	Pressure	Gravimetric		Volumetric[b]
	MPa	(wt.%)[a]	(mg g^{-1})	(mg cm^{-3})
MIL-53 Al	2	2.1	21.7	8.5
MOF-5	3	4.7	49.7	17.1
HKUST-1	2	3.8	39.9	14.9
MOF-177	3	6.1	65.2	17.2

Table S5. Excess H_2 uptake at 273 K and 14 MPa for the four MOFs.

Sample	**Excess H_2 uptake at 273 K and 14 MPa**		
	Gravimetric		Volumetric[b] [c]
	(wt.%) [a]	(mg g^{-1})	(mg cm^{-3})
MIL-53 Al	0.7	6.7	2.6
MOF-5	0.8	7.9	2.7
HKUST-1	1	10.1	3.8
MOF-177	1.1	10.8	2.9

Table S6. Results obtained from the linear regression of the excess H_2 plotted against the density of the gas phase in the saturation regime.

	Range of ρ_g [c]	R^2	V_a	y-intercept	ρ_a [d]
	(kg m^{-3})		(cm^3 g^{-1})	(mg g^{-1})	(kg m^{-3})

MOF177	25-40	0.9962	1.05	85	81
MOF-5	25-40	0.9975	0.59	62	105
HKUST-1	17-40	0.9993	0.46	45	99
MIL-53Al	17-40	0.9999	0.41	27	65

[a] H_2 uptake [wt%] calculated according to: $wt\% = \frac{mass\ of\ H2}{mass\ of\ H2 + mass\ of\ MOF} \times 100\%$.

[b] Volumetric uptake calculated based on the tapped density.

[c] Range in which the linear regression was performed.

[d] Obtained from the intercept with the *x*-axis of the extrapolated curve in **Figure 3c**.

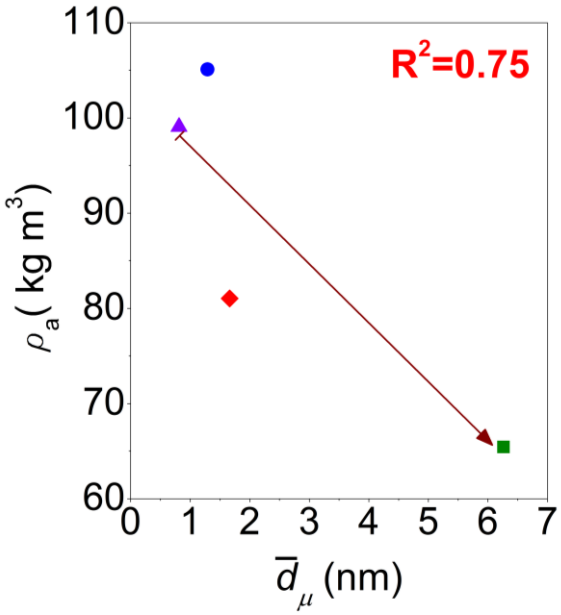

Figure S4. Density of the adsorbed phase as a function of average micropore size for MOF-177 ◆ , MOF-5 ● , MIL-53 Al ■ , and HKUST-1 ▲ .

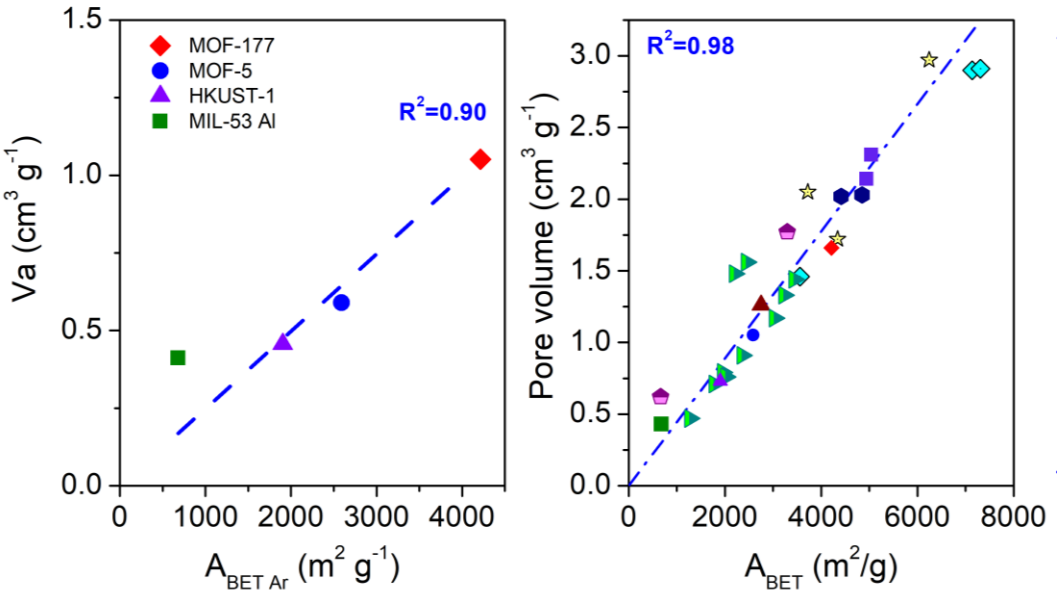

Figure S5. a) Evolution of V_a with A_{BET}. The V_a values correspond to those obtained from the linear regression of the excess H_2 uptake as a function of gas phase density (**Table S6**); b) Pore volume plotted against the A_{BET} of MOFs from the open literature: [11] [12] [13] [14] [15] [9] [16] and data reported in this study (◆ ● ■ ▲).

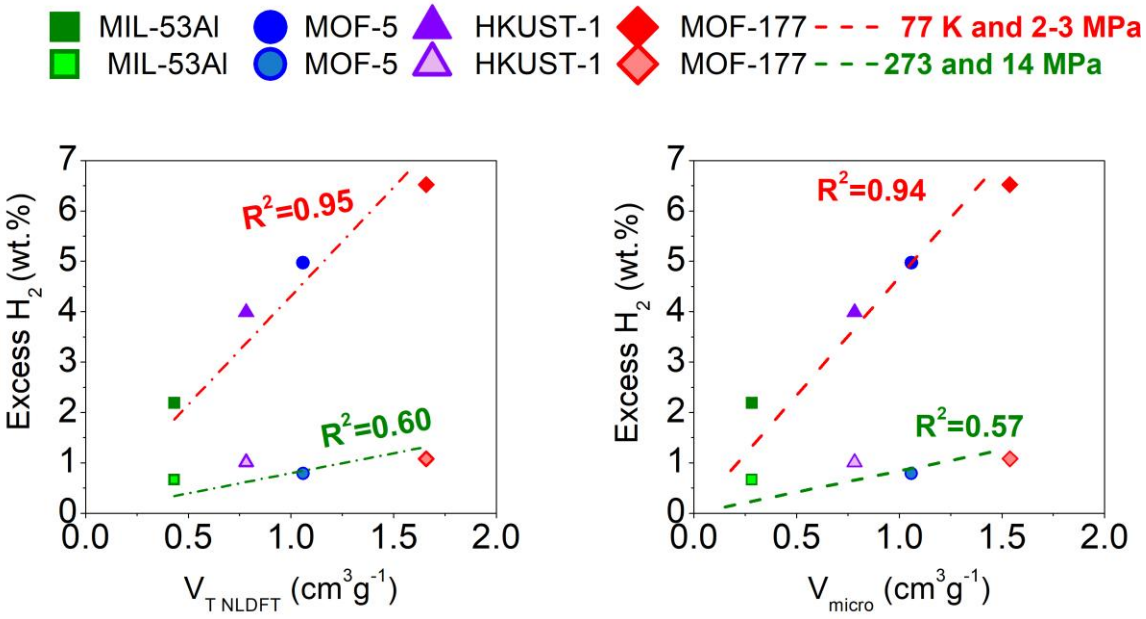

Figure S6. Excess hydrogen uptake at 77 K and 2-3MPa (■ MIL-53AL, ● MOF-5, ▲ HKUST-1, ◆ MOF-177 and ---) and 273 K and 14 MPa (□ MIL-53AL, ○ MOF-5, △ HKUST-1, ◇ MOF-177 and ---) as a function of: (a) total pore volume, $V_{T\ NLDFT}$; and (b) micropore volume, V_{micro}.

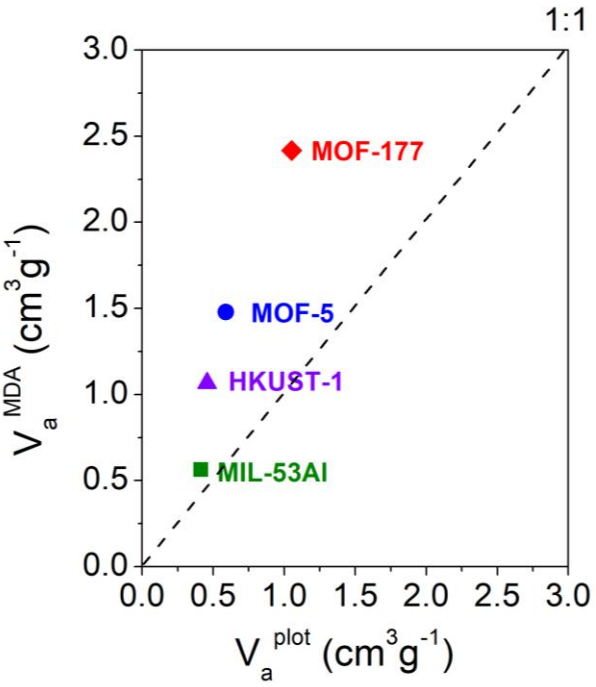

Figure S7. Adsorbed volume obtained from the fit of the MDA model, V_a^{MDA}, plotted as a function of V_a^{plot} obtained from **Figure 3c** for samples: ■ MIL-53AL, ● MOF-5, ▲ HKUST-1, and ◆ MOF-177.

Table S7. Textural properties and H_2 uptakes of different MOFs reported in the literature.

Sample	ρ_{cry} [a]	ρ_{sk} [b]	ρ_{TAP} [c]	$V_{T\ N2}$ [d]	$\bar{d}_T$ [e]	A_{BET} [f]	n_{exc} [g] at 77 K	Measurement pressure	n_{abs} [h] at 77 K
	g cm^{-3}	g cm^{-3}	g cm^{-3}	cm^3 g^{-1}	nm	m^2 g^{-1}	wt.%	MPa	wt.%
DUT-6	0.386 [11]	1.66[11]	0.23 [11]	2.02 [11]	1.2 [11]	4414 [11]	5.45 [11]	2.5	6.55 [17]
DUT-8(Co)	1.295 [11,12]	0.386[11]	0.29 [11]	0.62 [11]	-	6632 [11]	1.15 [12]	2.5	1.31 [17]
DUT-9	0.467 [18]	1.295 [11,12]	0.27 [11]	1.77 [18]	-	3293 [12]	5.24 [12]	2.5	5.97 [17]
DUT-23(Co)	0.403 [11]	1.42 [11]	0.23 [11]	2.03 [19]	1.2 [11]	4850 [11]	6.73 [11]	2.5	7.61 [17]
MFU-4(Co)	1.179 [17]	1.93 [12]	0.44 [11]	-	0.9 [11]	1350 [12]	2.85 [12]	2.5	3.26 [17]
Mg-Formate	1.398 [11]	1.68 [11]	0.59 [11]	-	0.34 [11]	357 [12]	0.68 [11]	2.5	0.77 [17]
MIL-53 Fe	0.690 [17]	2.03 [11]	0.43 [11]	-	-	1677 [12]	2.71 [11]	2.5	3.11 [11]
Fe-BTCGel	-	1.81 [12]	0.69 [11]	-	-	772 [12]	1.62 [11]	2.5	1.86 [17]
MFU-4I	0.560 [13]	-	-	1.26 [13]	-	2750 [13]	4.00 [13]	2.5	4.35 [17]
MOF-5	0.605 [20]	-	-	1.37 [17]	1.2 [11]	2360 [21]	4.48 [21]	2.5	4.80 [17]
MIL-101(Cr)	0.610 [22]	-	-	1.85 [11]	0.7 [11]	2761 [11]	-	2.5	5.01 [17]
MOF-177		-	-	1.69 [10]	1.1 [12]	5250 [10]	6.28 [12]	2	6.92 [a]
HKUST-1	0.650 [9]	-	-	-	0.5 [11]	1527 [11]/ 1980 [9]	3.55 [11]	2	3.92 [a]
DUT-4	-	-	-	-	0.9 [11]	1308 [11]	2.13 [11]	2	2.08 [17]
DUT-5	-	-	-	-	1.1 [11]	1613 [11]	3.19 [11]	2	3.09 [17]
PAF-1	-	1.12 [12]	0.138 [12]		-	3363 [12]	5.97 [12]	2.5	-
NU-1101	0.459 [14,23]	-	-	2.82 [24]	-	4340 [14]	5.7 [14]	3.76	7.66 [a]
NU-1102	0.40 [14,23]	-	-	-	-	3720 [14]	6.1 [14]	4.31	8.68 [a]
NU-1103	0.298 [14,23]	-	-	-	-	6245 [14]	7.0 [14]	4.88	11.01 [a]
NU-1501-Fe	0.299 [15]	-	-	2.9 [15]	1.5 [15]	7140 [15]	7.4 [15]	4	10.68 [a]
NU-1501-Al	0.283 [15]	-	-	2.91 [15]	1.5 [15]	7310 [15]	8.1 [15]	3.2	10.77 [a]
NU-1500-Al	0.498 [15]	-	-	1.46 [15]	1.4 [15]	3560 [15]	5.6 [15]	4	7.33 [a]
NU-100	0.290 [24]	-	-	2.82 [15]	-	6143 [15]	9.05 [24]	7	13.43 [a]
PCN-61	-	-	-	-	-	3000 [25]	5.9 [25]	3.3	-
PCN-66	-	-	-	-	-	4000 [25]	6.2 [25]	4.5	-
PCN-68	-	-	-	-	-	5109 [25]	6.8 [25]	5	-

[a] Single-crystal density obtained by XRD.
[b] Skeleton density obtained by He pycnometry.

[c] Tapped density.
[d] Total pore volumes determined from the N_2 adsorption isotherm at $p/p°$ in the range 0.97-0.99.
[e] The average pore size in [11] was calculated from the structural data of the material. The pore size distributions in [15] were determined based on the density functional theory (DFT) model with slit-shaped pores (N_2 DFT model).
[f] Brunauer-Emmett-Teller area.
[g] Excess uptake [wt.%] of H_2 calculated according to: $wt\% = \frac{mass\ of\ excess\ H2}{mass\ of\ excess\ H2 + mass\ of\ MOF} \times 100\%$.
[h] Absolute uptake, calculated from the excess data using REPROF software to calculate the density of H_2 gas and considering the volume of the adsorbed phase volume to be equal to $V_{T\,N2}$. The absolute uptake [wt.%] of H_2 was calculated according to: $wt\% = \frac{mass\ of\ absolute\ H2}{mass\ of\ absolute\ H2 + mass\ of\ MOF} \times 100\%$.

[i] Isosteric heat of H_2 adsorption.

Table S8. Absolute H_2 uptakes of different MOFs reported in the literature.

Sample	Pressure (MPa)	Gravimetric absolute H_2 uptake at 77 K [a] (mg g^{-1})	Volumetric absolute H_2 uptake at 77 K [b] ($\rho_{pack} = \rho_{cry}$) (g cm^{-3})	Volumetric absolute H_2 uptake at 77 K [c] ($\rho_{pack} = 0.74\ \rho_{cry}$) (g cm^{-3})	Volumetric absolute H_2 uptake at 77 K [d] ($\rho_{pack} = \rho_{TAP}$) (g cm^{-3})	Ref.
MIL-53-Al	2	25.5	24.9	18.4	10.0	This study
MOF-5	3	58.3	34.4	25.4	20.1	
HKUST-1	2	43.5	38.2	28.3	16.2	
MOF-177	3	78.5	33.8	25.0	20.8	
MSC30	4	58.5			14.6	26
MSP20X	4	48.0			16.8	
AX-21_33	2	53.2			14.0	27
AC-K5	2	41.6			25.4	28
AC-K3	2	32.5			21.8	
DUT-6	2.5	70.1	27.1	20.0	16.1	17
DUT-8(Co)	2.5	13.3	17.2	12.7	3.9	
DUT-9	2.5	63.5	29.7	21.9	17.1	
DUT-23(Co)	2.5	82.4	33.2	24.6	19.0	
MFU-4(Co)	2.5	33.7	39.7	29.4	14.8	
Mg-Formate	2.5	7.8	10.9	8.1	4.6	
MIL-53 Fe	2.5	32.1	22.1	16.4	13.8	
Fe-BTCGel	2.5	19.0	0.0		13.1	
MFU-4I	2.5	45.5	25.5	18.9		
MOF-5	2.5	50.4	30.5	22.6		
MIL-101(Cr)	2.5	52.7	32.1	23.8		
MOF-177	2	74.4	32.0	23.7		
HKUST-1	2	40.8	26.5	19.6		11
NU-1101	3.76	83.0	38.1	28.2		14

NU-1102	4.31	95.1	38.3	28.3		
NU-1103	4.88	123.8	36.9	27.3		
NU-1501-Fe	4	119.6	35.8	26.5		15
NU-1501-Al	3.2	120.7	34.2	25.3		
NU-1500-Al	4	79.1	39.4	29.2		

[a] Absolute uptake from excess reported data, calculated using the REPROF software to calculate the gas H_2 density and considering the adsorbed phase volume as the total pore volume.

[b] Volumetric uptake calculated based on the single-crystal density (reported in **Table S9**).

[c] Volumetric uptake calculated considering the packing density equal to 74 % of the single-crystal density.

[d] Volumetric uptake calculated based on the tapped density.

Table S9. DA parameters of each MOF, obtained by application of Eq (5) to H_2 adsorption at eleven different temperatures, from 77 to 273 K (fittings are shown in **Figure 5**). For comparison, the MDA parameters of CACs [29] are shown.

Sample		m	V_a ($cm^3\ g^{-1}$)	n_{max} ($mol\ kg^{-1}$)	α ($J\ mol^{-1}$)	β ($J\ mol^{-1}\ K^{-1}$)	P_0 (MPa)	Average R^2	Reference
MOFs	**MIL-53 Al**	1.95	0.56	20.31	3562	5.46	130	0.96	This study
	MOF-5	2.11	1.48	77.98	2525	16.51	823	0.97	
	HKUST-1	1.65	1.07	43.84	3438	4.92	172	0.98	
	MOF-177	2.25	2.42	115.67	2251	19.46	976	0.97	
CACs	**MSC30**	2.00	1.50	72.5	3300	15.80	1013	0.99	29
	SA20	2.00	0.72	36.7	3244	13.69	616	0.99	
	SA1500	2.00	0.87	46.2	3345	13.08	632	0.98	
	MSP20X	2.00	1.09	47.4	4094	11.50	632	0.99	
	TH90I	2.00	0.56	24.5	4699	9.72	655	0.96	
	Filtrasorb400	2.00	0.36	20.8	4300	9.75	700	0.97	

Table S 10. Determination coefficient obtained when linearly fitting MDA parameters to textural parameters. The best fits are in bold and dark green and the worst fits in red.

		$V_{T,\ NLDFT}$ ($cm^3\ g^{-1}$)	V_{micro} ($cm^3\ g^{-1}$)	$V_{(<0.7nm)}$ ($cm^3\ g^{-1}$)	$\bar{d}_T$ (nm)	$\bar{d}_\mu$ (nm)	$\bar{d}_{(<0.7nm)}$ (nm)	S_{NLDFT} ($m^2\ g^{-1}$)	A_{BET} ($m^2\ g^{-1}$)
Parameters of the Modified Dubinin-Astakhov equation	P_0	0.45	0.36	0.25	0.18	0.64	0.11	0.00	0.49
	P_0 (MOFs only)	**0.82**	0.81	**0.96**	0.24	**0.96**	**0.95**	0.22	**0.80**
	n_{max}	0.68	**0.95**	0.49	0.21	0.72	0.35	0.54	**0.94**
	V_a	0.64	**0.95**	0.42	0.19	0.61	0.36	0.62	**0.91**
	β	0.68	0.54	0.55	0.10	**0.93**	0.36	0.06	0.67
	α (only MOFs)	**0.85**	0.85	**0.94**	0.27	**0.97**	**0.96**	0.26	0.84
	α (only CACs)	**0.84**	0.17	**0.86**	0.31	**0.97**	0.12	0.19	0.43
	m	0.21	0.23	0.28	0.00	0.57	0.25	0.00	0.25
	m (only MOFs)	0.47	0.38	**0.88**	0.37	**0.96**	0.51	0.00	0.41

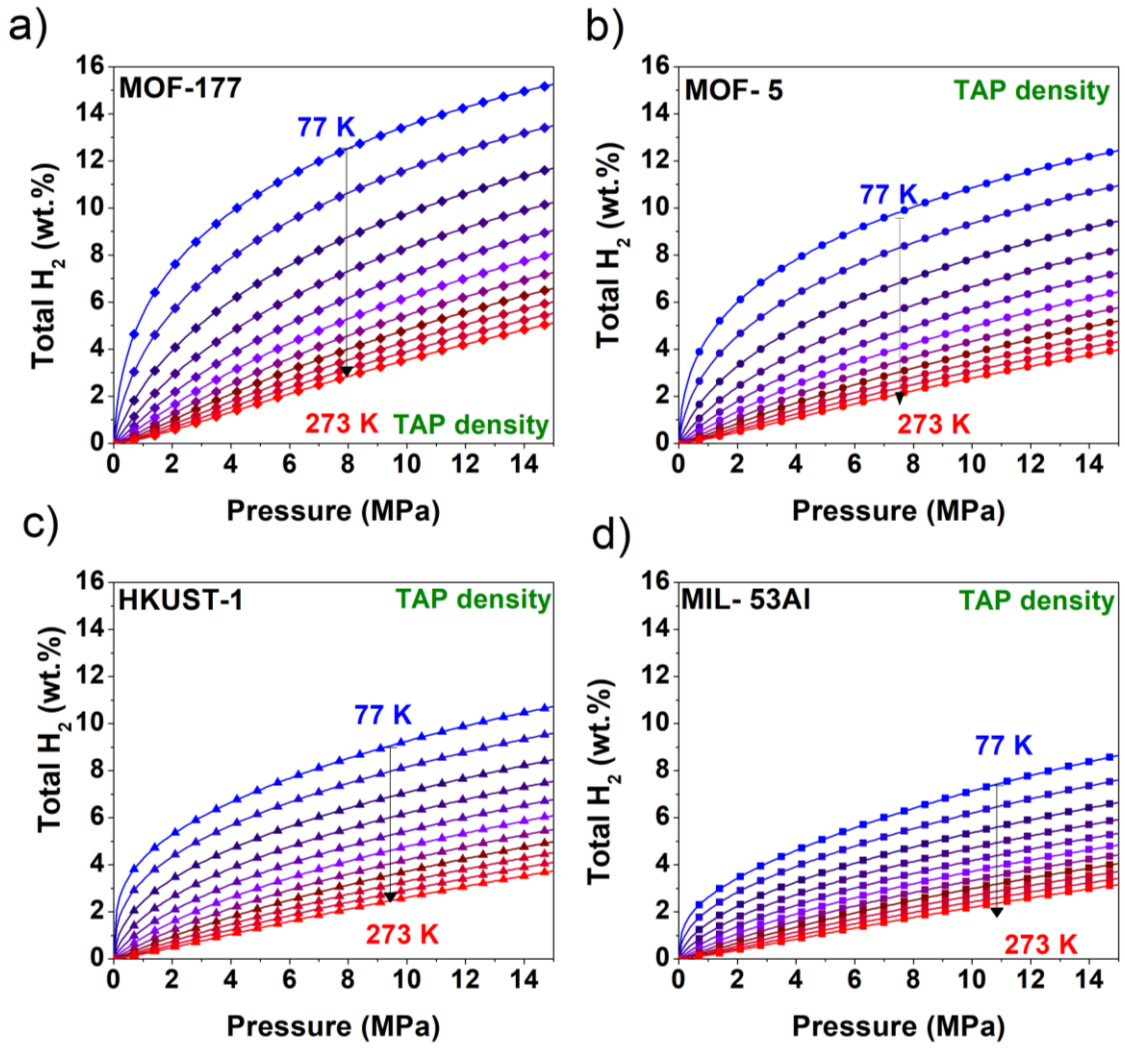

Figure S8. Total hydrogen adsorption isotherms calculated using the tapped density for the MOFs: (a) MOF-177, (b) MOF-5, (c) HKUST-1, and (d) MIL-53 Al.

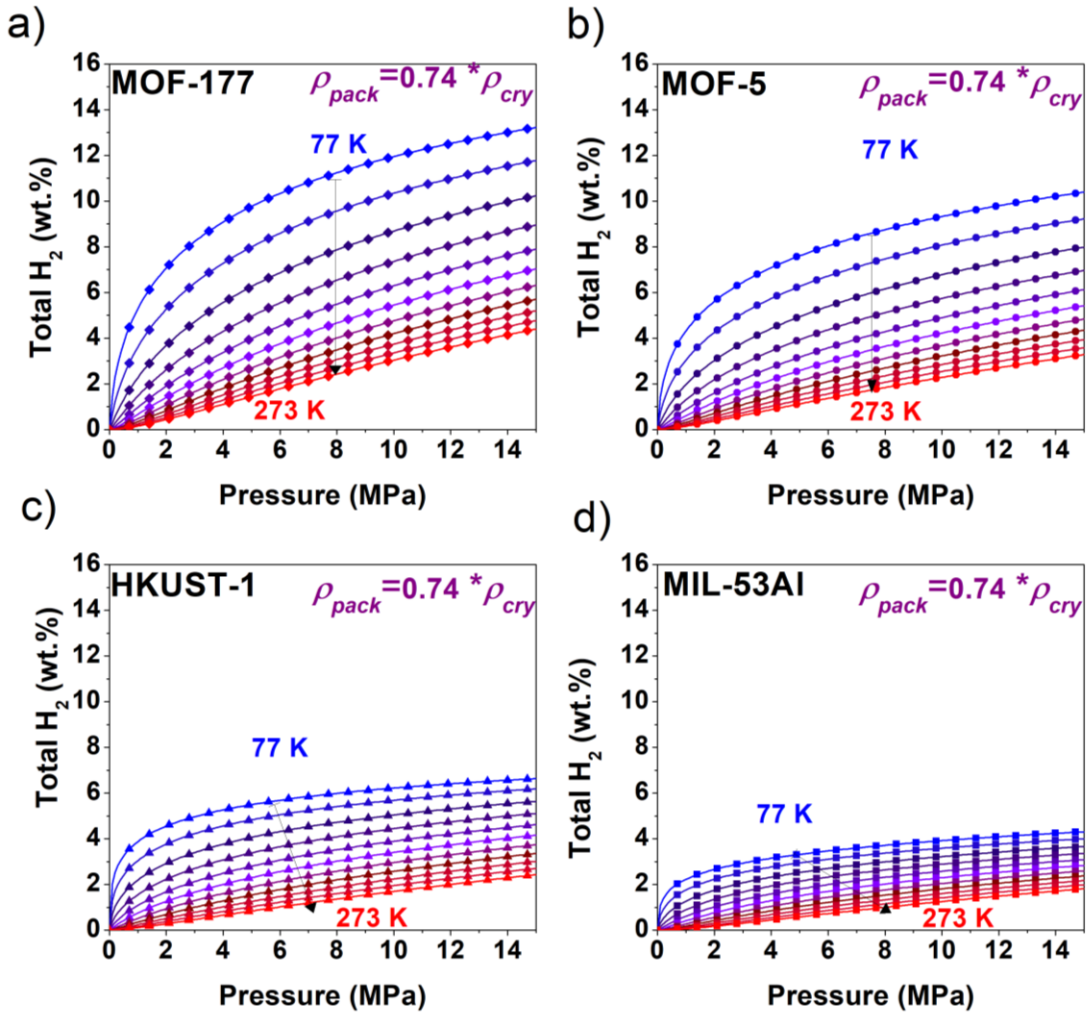

Figure S9. Same as Figure S8, but the assumption that the packing density is ρ_{pack} = 0.74 ρ_{cry}.

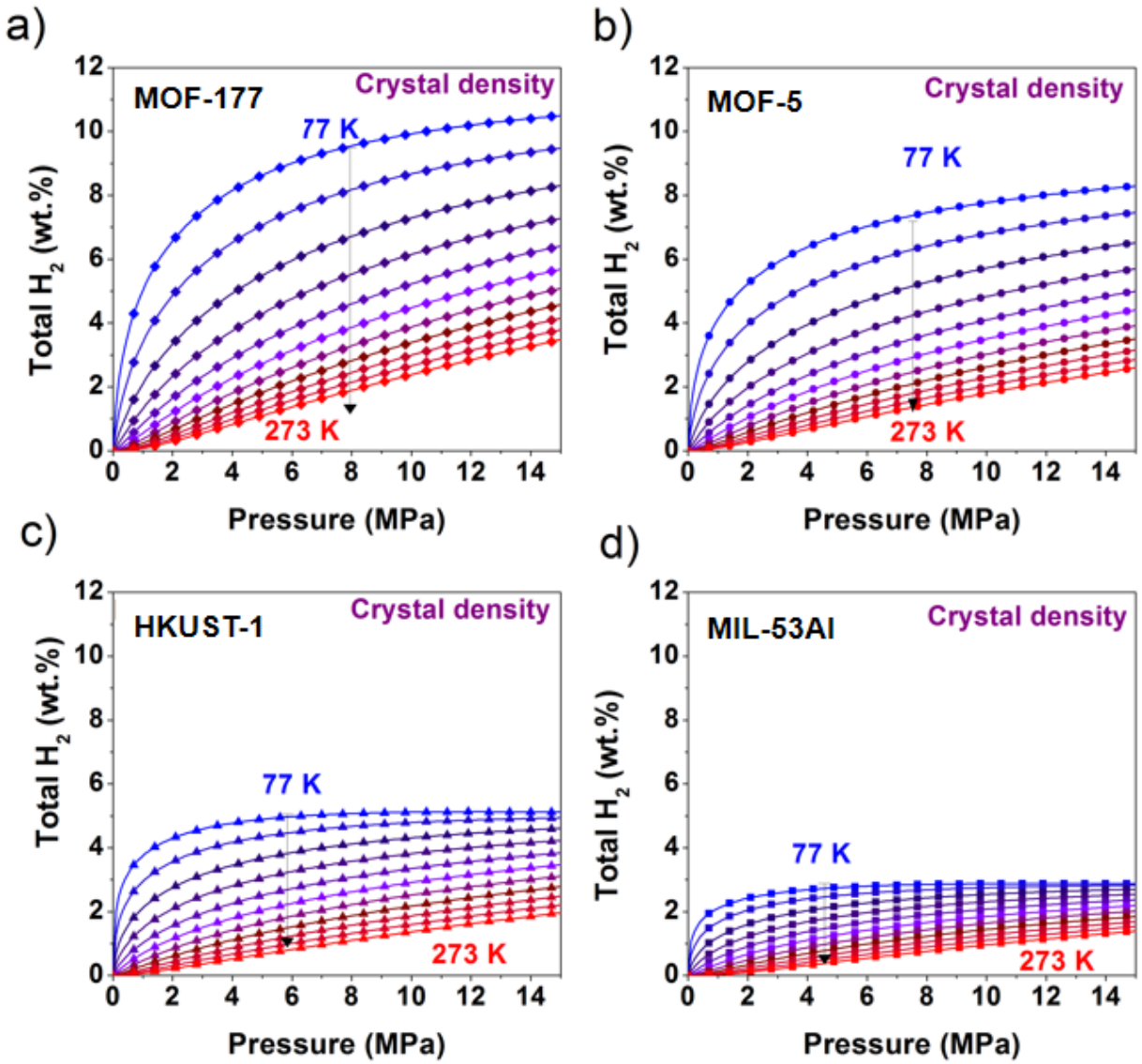

Figure S10. Same as Figure S8, but using the single-crystal density.

Table S11. Excess H_2 employed for calculating the H_2 release capacity when considering $\rho_{pack} = \rho_{cry}$ reported in recent studies.

Materials	A_{BET} [a]	V_T [b]	ρ_{cry} [c]	n_{exc} [d] at 77 K and 10 MPa	n_{exc} [e] at 77 K and 0.5 MPa	n_{exc} [f] at 160 K and 0.5 MPa	n_{tot} [g] at 77 K and 10 MPa	Δn_{H2} [h] 77 K/10MPa →77 K/0.5 MPa (crystal density)		Δn_{H2} [i] 77 K/10 MPa→160 K/0.5 MPa ($\rho_{pack} = \rho_{crys}$)		Ref.
	($m^2\ g^{-1}$)	($cm^3\ g^{-1}$)	($g\ cm^{-3}$)	(wt.%)	(wt.%)	(wt.%)	(wt.%)	(wt.%)	($mg\ cm^{-3}$)	(wt.%)	($mg\ cm^{-3}$)	
MIL53-Al	681	0.43	0.978 [6]	1.7	1.7	0.2	2.9	1.1	11.2	2.6	26.2	This study
MOF-5	2589	1.06	0.590 [7,8]	4.5	2.9	0.2	7.8	4.9	30.6	7.5	47.6	
HKUST-1	1903	0.78	0.879 [9]	3.1	3.1	0.5	5.1	2.1	18.4	4.6	42.2	
MOF-177	4215	1.66	0.430 [8,10,11]	5.3	3.4	0.2	9.9	6.7	31.1	9.7	45.7	
MSC30	3305	1.60	-	4.6	4.1	0.6						26
MSP20X	2363	0.94	-	2.8	2.6	0.2						
NU-1101	4340	1.72	0.459	4.8	3.7	0.3	9.5	6.1	31.0	9.1	47.0	14
NU-1102	3720	1.65	0.403	5.5	3.3	0.3	10.0	6.9	31.0	9.6	44.0	
NU-1103	6245	2.72	0.298	6.1	3.2	0.3	13.2	10.1	33.0	12.6	43.0	
NU-1500-Al	3560	1.46	0.498	4.5	3.8	0.3	8.6	4.8		8.2	44.6	15
NU-1501-Fe	7140	2.90	0.299	6.4	3.7	0.4	13.7	10.3		13.2	45.6	
NU-1501-Al	7310	2.91	0.283	7.2	4.0	0.3	14.4	11.1		14	46.2	
MOF-5	3510	1.36	0.590							7.8	51.9	30
NU-100	6050	3.17	0.290	6.6	3.7	0.3				13.9	47.6	9
HKUST-1	1980	0.75	0.881	3.1	3.5	0.4	5.3	1.9	17.0	4.9	46.0	
IRMOF-20	4070	1.65	0.510	5.2	3.4	0.3				9.1	51.0	
TT-112	3440	1.44	0.446					5.3	24.0	8.3	41.0	
NU-125	3230	1.33	0.578	4.8	4.6	0.5	8.2	4.1	24.0	7.8	49.0	
rht-MOF-7	1950	0.79	0.789	2.6	3.2	0.4	4.9	1.8	14.0	4.5	37.0	
Cu-MOF-74	1270	0.47	1.323	1.7	2.2	0.3	3.2	1.0	13.0	2.9	39.0	
PCN-250	1780	0.71	0.896	3.3	3.7	0.4	5.4	1.8	16.0	2.9	47.0	
NU-1000	2200	1.48	0.571					5.2	30.0	2.9	48.0	
UiO-67	2360	0.91	0.688					2.9	20.0	2.9	41.0	
UiO-68-Ant	3030	1.17	0.607					4.3	26.0	7.2	47.0	
CYCU-3-Al	2450	1.56	0.477	4.0	3.3	0.3	8.4	5.5	27.0	8	41.0	
NOTT-112	3440	1.84	0.446	5.0	3.9	0.4	8.8	5.3	25.0	9.1	41.0	
SNU-70	4940	2.14	0.411	5.6	3.2	0.2	10.8			10.6	47.9	16
UMCM-9	5040	2.31	0.370	5.9	3.5	0.3	11.5			11.3	47.4	

DUT-23(Co)	4850		0.403 [11]	6.3	4.3	3.1						31

[a] Brunauer-Emmett-Teller area.
[b] Total pore volumes determined from the N_2 adsorption isotherm at $p/p°$ in the range 0.97-0.99.
[c] Single-crystal density obtained by XRD.
[d] H_2 excess uptake reported in the literature at 77 K and 10 MPa.
[e] H_2 excess uptake reported in the literature at 77 K and 0.5 MPa.
[f] H_2 excess uptake reported in the literature at 160 K and 0.5 MPa.
[g] Reported H_2 total uptake at 77 K and 10 MPa. The data were calculated considering $\rho_{pack} = \rho_{crys}$
[h] Release capacity of a system loading at 77 K and 10 MPa and discharging at 77 K and 0.5 MPa reported in recent studies. The release capacities were calculated considering: $\rho_{pack} = \rho_{crys}$.
[i] Release capacity of a system loading at 77 K and 10 MPa and discharging at 160 K and 0.5 MPa reported in recent studies. The release capacities were calculated considering: $\rho_{pack} = \rho_{crys}$.

Table S12. H_2 release capacity Δn_{H2} calculated employing the single crystal density and the TAP density of MOFs reported in recent studies.

Materials	ρ_{TAP} [a]	ρ_{cry} [b]	ρ_{sk} [c]	$\rho_{pack} = 0.74\ \rho_{cry}$					$\rho_{pack} = \rho_{TAP}$					Ref.
				n_{tot} [e] at 77 K and 10 MPa	Δn_{H2} [f] 77 K/10MPa →77 K/0.5 MPa		Δn_{H2} [g] 77 K/10 MPa→160 K/0.5 MPa		n_{tot} [h] at 77 K and 10 MPa	Δn_{H2} [i] 77 K/10MPa →77 K/0.5 MPa		Δn_{H2} [j] 77 K/10 MPa→160 K/0.5 MPa		
	(g cm^{-3})	(g cm^{-3})	(g cm^{-3})	(wt.%)	(wt.%)	(mg cm^{-3})	(wt.%)	(mg cm^{-3})	(wt.%)	(wt.%)	(mg cm^{-3})	(wt.%)	(mg cm^{-3})	
MIL53-Al	0.394	0.978 [6]	1.6 [c]	4.0	2.2	16.1	3.7	27.5	7.4	5.3	22.1	6.8	28.9	This study
MOF-5	0.345	0.590 [7,8]	2.0 [c]	9.8	6.5	30.6	9.0	43.3	11.5	8.3	31.1	10.5	40.6	
HKUST-1	0.373	0.879 [9]	2.2 [c]	6.4	3.2	21.5	5.7	39.5	9.7	6.2	24.7	8.7	35.7	
MOF-177	0.264	0.430 [8,10,11]	1.7 [c]	12.7	8.8	30.9	11.7	42.0	14.5	10.3	30.4	13.2	40.1	
MSC30	0.25		2.5 [c]						14.9	10.1	28.1	13.2	38.1	26
MSP20X	0.35		2.4 [c]						10.0	6.9	25.9	9.1	35.2	
NU-1101		0.459	2.4 [d]	12.2	8.0	29.6	11.1	42.2						14
NU-1102		0.403	1.3 [d]	13.0	9.1	30.0	11.8	39.8						
NU-1103		0.298	1.6 [d]	17.2	13.0	32.9	15.4	40.1						
NU-1500-Al		0.498	1.9 [d]	11.0	6.8	26.7	10.0	40.8						15
NU-1501-Fe		0.299	2.2 [d]	17.8	13.1	33.2	15.9	41.8						
NU-1501-Al		0.283	1.6 [d]	18.8	13.8	33.4	16.8	42.2						
HKUST-1	0.373	0.881	2.2 [c]	6.4	2.8	18.5	5.8	40.1	9.7			8.8	36.0	9
NU-125		0.578	2.2 [d]	10.3	5.5	24.7	9.2	43.6						
rht-MOF-7		0.789	2.2 [d]	6.4	3.0	18.2	5.8	35.6						
Cu-MOF-74		1.323	2.7 [d]	3.7	1.4	14.3	3.3	33.7						
PCN-250		0.896	2.5 [d]	6.7	2.8	19.2	6.1	42.8						
NOTT-112		0.446	1.2 [d]	11.4	7.2	25.4	10.3	38.0						
CYCU-3-Al		0.477	2.0 [d]	10.8	7.1	27.2	9.9	38.7						
SNU-70		0.411	2.1 [d]	13.7	9.9	33.3	12.5	43.5						31
IRMOF-20		0.510	2.4 [c 16]	11.7	7.9	32.4	10.7	45.1						

DUT-23(Co)	0.230	0.403 [11]	1.4 [c 11]	13.9	9.1	30.0	10.3	34.4	16.6			13.2	35.0	

[a] Tap density
[b] Single-crystal density obtained by XRD.
[c] Skeleton density measured by He pycnometry.
[d] When the skeleton density, ρ_{sk} [kg m^{-3}], was not reported, it was estimated according equation (Eq.(10)) as follows:

$$\rho_{skel} = \left(\frac{n_{exc} - n_{tot}}{\rho_{gas}} + \frac{1}{\rho_{cry}} \right)^{-1}$$

where n_{exc} [mol kg^{-1}] and n_{tot} [mol kg^{-1}] are the excess and total uptake reported at 77 K and 10 MPa (Table S10), ρ_{cry} [kg m^{-3}] is the single-crystal density and ρ_g [mol m^{-3}] is the gas phase density obtained from the REFPROP-7 software.

[e] Calculated H_2 total uptake at 77 K and 10 MPa. The data were calculated considering $\rho_{pack} = 0.74\rho_{crys}$
[f] Release capacity of a system loaded at 77 K and 10 MPa and discharged at 77 K and 0.5 MPa. The release capacities were calculated considering: $\rho_{pack} = 0.74\,\rho_{crys}$.
[g] Release capacity of a system loaded at 77 K and 10 MPa and discharged at 160 K and 0.5 MPa. The release capacities were calculated considering: $\rho_{pack} = 0.74\,\rho_{cry}$.
[h] Calculated H_2 total uptake at 77 K and 10 MPa. The data were calculated considering $\rho_{pack} = \rho_{TAP}$
[i] Release capacity of a system loaded at 77 K and 10 MPa and discharged at 77 K and 0.5 MPa reported in recent studies. The release capacities were calculated considering: $\rho_{pack} = \rho_{TAP}$.
[j] Release capacity of a system loaded at 77 K and 10 MPa and discharged at 160 K and 0.5 MPa reported in recent studies. The release capacities were calculated considering: $\rho_{pack} = \rho_{TAP}$.

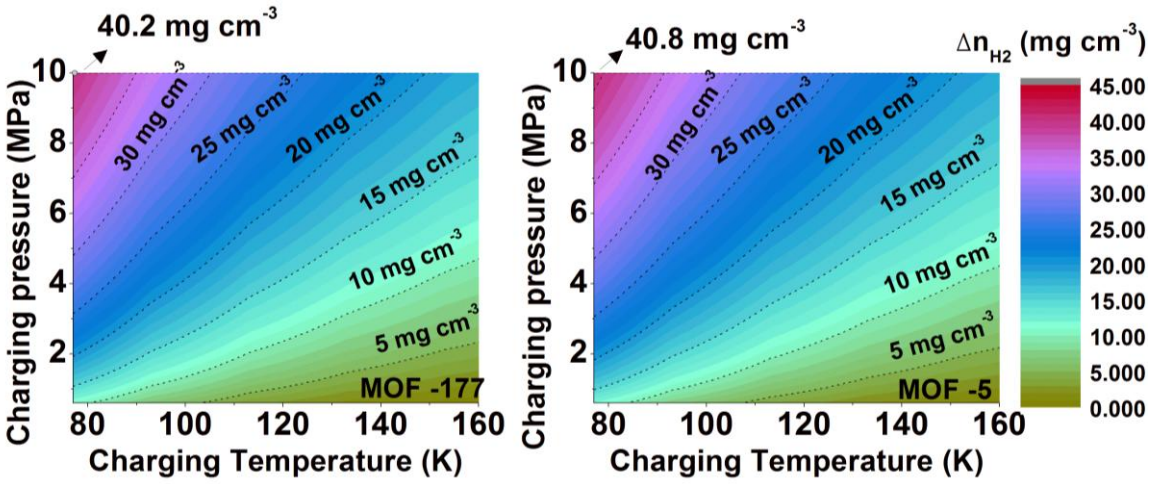

Figure S11. Volumetric release capacity profile as a function of the charging temperature and pressure, with discharge pressure and temperature equal to 0.5 MPa and 160 K, respectively for: MOF-177 (a); and MOF-5 (b).

References

(1) Gómez-Gualdrón, D. A.; Moghadam, P. Z.; Hupp, J. T.; Farha, O. K.; Snurr, R. Q. Application of Consistency Criteria To Calculate BET Areas of Micro- And Mesoporous Metal–Organic Frameworks. *J. Am. Chem. Soc.* **2016**, *138* (1), 215–224. https://doi.org/10.1021/jacs.5b10266.

(2) Kapoor, A.; Ritter, J. A.; Yang, R. T. On the Dubinin-Radushkevich Equation for Adsorption in Microporous Solids in the Henry's Law Region. *Langmuir* **1989**, *5* (4), 1118–1121. https://doi.org/10.1021/la00088a043.

(3) Rabbani, M. G.; Sekizkardes, A. K.; Kahveci, Z.; Reich, T. E.; Ding, R.; El-Kaderi, H. M. A 2D Mesoporous Imine-Linked Covalent Organic Framework for High Pressure Gas Storage Applications. *Chemistry – A European Journal* **2013**, *19* (10), 3324–3328. https://doi.org/10.1002/chem.201203753.

(4) Moellmer, J.; Celer, E. B.; Luebke, R.; Cairns, A. J.; Staudt, R.; Eddaoudi, M.; Thommes, M. Insights on Adsorption Characterization of Metal-Organic Frameworks: A Benchmark Study on the Novel Soc-MOF. *Microporous and Mesoporous Materials* **2010**, *129* (3), 345–353. https://doi.org/10.1016/j.micromeso.2009.06.014.

(5) Jagiello, J.; Kenvin, J.; Ania, C. O.; Parra, J. B.; Celzard, A.; Fierro, V. Exploiting the Adsorption of Simple Gases O2 and H2 with Minimal Quadrupole Moments for the Dual Gas Characterization of Nanoporous Carbons Using 2D-NLDFT Models. *Carbon* **2020**, *160*, 164–175. https://doi.org/10.1016/j.carbon.2020.01.013.

(6) Kim, S.-Y.; Kang, J. H.; Kim, S.-I.; Bae, Y.-S. Extraordinarily Large and Stable Methane Delivery of MIL-53(Al) under LNG-ANG Conditions. *Chemical Engineering Journal* **2019**, *365*, 242–248. https://doi.org/10.1016/j.cej.2019.01.182.

(7) Li, H.; Eddaoudi, M.; O'Keeffe, M.; Yaghi, O. M. Design and Synthesis of an Exceptionally Stable and Highly Porous Metal-Organic Framework. **1999**, *402*, 4.
(8) Furukawa, H.; Ko, N.; Go, Y. B.; Aratani, N.; Choi, S. B.; Choi, E.; Yazaydin, A. O.; Snurr, R. Q.; O'Keeffe, M.; Kim, J.; Yaghi, O. M. Ultrahigh Porosity in Metal-Organic Frameworks. *Science* **2010**, *329* (5990), 424–428. https://doi.org/10.1126/science.1192160.
(9) García-Holley, P.; Schweitzer, B.; Islamoglu, T.; Liu, Y.; Lin, L.; Rodriguez, S.; Weston, M. H.; Hupp, J. T.; Gómez-Gualdrón, D. A.; Yildirim, T.; Farha, O. K. Benchmark Study of Hydrogen Storage in Metal–Organic Frameworks under Temperature and Pressure Swing Conditions. *ACS Energy Lett.* **2018**, *3* (3), 748–754. https://doi.org/10.1021/acsenergylett.8b00154.
(10) Furukawa, H.; Miller, M. A.; Yaghi, O. M. Independent Verification of the Saturation Hydrogen Uptake in MOF-177 and Establishment of a Benchmark for Hydrogen Adsorption in Metal–Organic Frameworks. *J. Mater. Chem.* **2007**, *17* (30), 3197. https://doi.org/10.1039/b703608f.
(11) Schlichtenmayer, M.; Hirscher, M. Nanosponges for Hydrogen Storage. *J. Mater. Chem.* **2012**, *22* (20), 10134. https://doi.org/10.1039/c2jm15890f.
(12) Schlichtenmayer, M.; Hirscher, M. The Usable Capacity of Porous Materials for Hydrogen Storage. *Appl. Phys. A* **2016**, *122* (4), 379. https://doi.org/10.1007/s00339-016-9864-6.
(13) Denysenko, D.; Grzywa, M.; Tonigold, M.; Streppel, B.; Krkljus, I.; Hirscher, M.; Mugnaioli, E.; Kolb, U.; Hanss, J.; Volkmer, D. Elucidating Gating Effects for Hydrogen Sorption in MFU-4-Type Triazolate-Based Metal-Organic Frameworks Featuring Different Pore Sizes. *Chem. Eur. J.* **2011**, *17* (6), 1837–1848. https://doi.org/10.1002/chem.201001872.
(14) Gómez-Gualdrón, D. A.; Wang, T. C.; García-Holley, P.; Sawelewa, R. M.; Argueta, E.; Snurr, R. Q.; Hupp, J. T.; Yildirim, T.; Farha, O. K. Understanding Volumetric and Gravimetric Hydrogen Adsorption Trade-off in Metal–Organic Frameworks. *ACS Appl. Mater. Interfaces* **2017**, *9* (39), 33419–33428. https://doi.org/10.1021/acsami.7b01190.
(15) Chen, Z.; Li, P.; Anderson, R.; Wang, X.; Zhang, X.; Robison, L.; Redfern, L. R.; Moribe, S.; Islamoglu, T.; Gómez-Gualdrón, D. A.; Yildirim, T.; Stoddart, J. F.; Farha, O. K. Balancing Volumetric and Gravimetric Uptake in Highly Porous Materials for Clean Energy. *Science* **2020**, *368* (6488), 8. https://doi.org/10.1126/science.aaz8881.
(16) Ahmed, A.; Seth, S.; Purewal, J.; Wong-Foy, A. G.; Veenstra, M.; Matzger, A. J.; Siegel, D. J. Exceptional Hydrogen Storage Achieved by Screening Nearly Half a Million Metal-Organic Frameworks. *Nat Commun* **2019**, *10* (1), 1568. https://doi.org/10.1038/s41467-019-09365-w.
(17) Balderas- Xicohténcatl, R.; Schlichtenmayer, M.; Hirscher, M. Volumetric Hydrogen Storage Capacity in Metal–Organic Frameworks. *Energy Technology* **2018**, *6* (3), 578–582. https://doi.org/10.1002/ente.201700636.
(18) Gedrich, K.; Senkovska, I.; Klein, N.; Stoeck, U.; Henschel, A.; Lohe, M. R.; Baburin, I. A.; Mueller, U.; Kaskel, S. A Highly Porous Metal–Organic Framework with Open Nickel Sites. *Angewandte Chemie International Edition* **2010**, *49* (45), 8489–8492. https://doi.org/10.1002/anie.201001735.

(19) Klein, N.; Senkovska, I.; Baburin, I. A.; Grünker, R.; Stoeck, U.; Schlichtenmayer, M.; Streppel, B.; Mueller, U.; Leoni, S.; Hirscher, M.; Kaskel, S. Route to a Family of Robust, Non-Interpenetrated Metal–Organic Frameworks with Pto-like Topology. *Chemistry – A European Journal* **2011**, *17* (46), 13007–13016. https://doi.org/10.1002/chem.201101383.

(20) Purewal, J. J.; Liu, D.; Yang, J.; Sudik, A.; Siegel, D. J.; Maurer, S.; Müller, U. Increased Volumetric Hydrogen Uptake of MOF-5 by Powder Densification. *International Journal of Hydrogen Energy* **2012**, *37* (3), 2723–2727. https://doi.org/10.1016/j.ijhydene.2011.03.002.

(21) Schmitz, B.; Müller, U.; Trukhan, N.; Schubert, M.; Férey, G.; Hirscher, M. Heat of Adsorption for Hydrogen in Microporous High-Surface-Area Materials. *Chemphyschem* **2008**, *9* (15), 2181–2184. https://doi.org/10.1002/cphc.200800463.

(22) Dybtsev, D.; Serre, C.; Schmitz, B.; Panella, B.; Hirscher, M.; Latroche, M.; Llewellyn, P. L.; Cordier, S.; Molard, Y.; Haouas, M.; Taulelle, F.; Férey, G. Influence of $[Mo_6Br_8F_6]^{2-}$ Cluster Unit Inclusion within the Mesoporous Solid MIL-101 on Hydrogen Storage Performance. *Langmuir* **2010**, *26* (13), 11283–11290. https://doi.org/10.1021/la100601a.

(23) Wang, T. C.; Bury, W.; Gómez-Gualdrón, D. A.; Vermeulen, N. A.; Mondloch, J. E.; Deria, P.; Zhang, K.; Moghadam, P. Z.; Sarjeant, A. A.; Snurr, R. Q.; Stoddart, J. F.; Hupp, J. T.; Farha, O. K. Ultrahigh Surface Area Zirconium MOFs and Insights into the Applicability of the BET Theory. *J. Am. Chem. Soc.* **2015**, *137* (10), 3585–3591. https://doi.org/10.1021/ja512973b.

(24) Farha, O. K.; Özgür Yazaydın, A.; Eryazici, I.; Malliakas, C. D.; Hauser, B. G.; Kanatzidis, M. G.; Nguyen, S. T.; Snurr, R. Q.; Hupp, J. T. De Novo Synthesis of a Metal–Organic Framework Material Featuring Ultrahigh Surface Area and Gas Storage Capacities. *Nature Chemistry* **2010**, *2*, 944.

(25) Yuan, D.; Zhao, D.; Sun, D.; Zhou, H.-C. An Isoreticular Series of Metal–Organic Frameworks with Dendritic Hexacarboxylate Ligands and Exceptionally High Gas-Uptake Capacity. *Angewandte Chemie International Edition* **2010**, *49* (31), 5357–5361. https://doi.org/10.1002/anie.201001009.

(26) Sdanghi, G.; Schaefer, S.; Maranzana, G.; Celzard, A.; Fierro, V. Application of the Modified Dubinin-Astakhov Equation for a Better Understanding of High-Pressure Hydrogen Adsorption on Activated Carbons. *International Journal of Hydrogen Energy* **2020**, *45* (48), 25912–25926. https://doi.org/10.1016/j.ijhydene.2019.09.240.

(27) Schlichtenmayer, M.; Streppel, B.; Hirscher, M. Hydrogen Physisorption in High SSA Microporous Materials – A Comparison between AX-21_33 and MOF-177 at Cryogenic Conditions. *International Journal of Hydrogen Energy* **2011**, *36* (1), 586–591. https://doi.org/10.1016/j.ijhydene.2010.09.057.

(28) Wang, H.; Gao, Q.; Hu, J. High Hydrogen Storage Capacity of Porous Carbons Prepared by Using Activated Carbon. *J. Am. Chem. Soc.* **2009**, *131* (20), 7016–7022. https://doi.org/10.1021/ja8083225.

(29) Ramirez-Vidal, P.; Canevesi, R. L. S.; Sdanghi, G.; Schaefer, S.; Maranzana, G.; Celzard, A.; Fierro, V. A Step Forward in Understanding the Hydrogen Adsorption and Compression on Activated Carbons. *ACS Appl. Mater. Interfaces* **2021**, *13* (10), 12562–12574. https://doi.org/10.1021/acsami.0c22192.

(30) Ahmed, A.; Liu, Y.; Purewal, J.; Tran, L. D.; Wong-Foy, A. G.; Veenstra, M.; Matzger, A. J.; Siegel, D. J. Balancing Gravimetric and Volumetric Hydrogen

Density in MOFs. *Energy Environ. Sci.* **2017**, *10* (11), 2459–2471. https://doi.org/10.1039/C7EE02477K.

(31) Purewal, J.; Veenstra, M.; Tamburello, D.; Ahmed, A.; Matzger, A. J.; Wong-Foy, A. G.; Seth, S.; Liu, Y.; Siegel, D. J. Estimation of System-Level Hydrogen Storage for Metal-Organic Frameworks with High Volumetric Storage Density. *International Journal of Hydrogen Energy* **2019**, *44* (29), 15135–15145. https://doi.org/10.1016/j.ijhydene.2019.04.082.